

TEST OF TIME-REVERSAL INVARIANCE IN THE BETA DECAY OF $\text{Ne}^{19}\dagger$

Frank P. Calaprice, Eugene D. Commins,* Hyatt M. Gibbs, and Gerald L. Wick
Physics Department and Lawrence Radiation Laboratory, University of California, Berkeley, California

and

David A. Dobson
Lawrence Radiation Laboratory, Livermore, California
(Received 12 April 1967)

The discovery of CP -invariance violation in K_2 decay¹ has stimulated widespread interest in the question of time-reversal (T) invariance and its possible violation in weak decays.² We report a test of T invariance in the mirror beta decay $\text{Ne}^{19} \rightarrow \text{F}^{19} + e^+ + \nu$ ($\tau_{1/2} = 18.5$ sec). Our experimental result gives no evidence for T -invariance violation.

The differential rate $d\lambda$ for an allowed beta transition with $I = I' = \frac{1}{2}$ (e.g., $\text{Ne}^{19} \rightarrow \text{F}^{19}$, or $n \rightarrow p$), when summed over electron polarizations, is given by the following theoretical formula³:

$$d\lambda = \frac{F(\mp Z, E) p^2 q^2 dp d\Omega_e d\Omega_\nu}{2(2\pi)^5 \hbar^7 c} \times \xi \left\{ 1 + a \frac{\vec{v}}{c} \cdot \hat{q} + \frac{\langle \vec{I} \rangle}{I} \cdot \left[A \frac{\vec{v}}{c} + B \hat{q} + D \left(\frac{\vec{v}}{c} \times \hat{q} \right) \right] \right\}. \quad (1)$$

Here, $F(\mp Z, E)$ is the Fermi function⁴; p , v , and E are the magnitude of the momentum, velocity, and energy, respectively, of the electron; $q = c^{-1}(E_{\text{max}} - E)$ is the magnitude of neutrino momentum and \hat{q} is a unit vector in its direction; and $d\Omega_e$ and $d\Omega_\nu$ are differential solid angles for the electron and neutrino, respectively. The spin polarization of the initial nucleus is specified by $\langle \vec{I} \rangle / I$. In Eq. (1), and in the following, + (-) refers to positron (neutron) emission. The quantities ξ , A , B , and D are given by

$$\xi = |C_\nu|^2 |\langle 1 \rangle|^2 + |C_A|^2 |\langle \sigma \rangle|^2, \quad (2)$$

$$A\xi = \pm \frac{2}{3} |C_A|^2 |\langle \sigma \rangle|^2 - 3^{-1/2} (C_V C_A^* + C_A C_V^*) \langle 1 \rangle \langle \sigma \rangle, \quad (3)$$

$$B\xi = \mp \frac{2}{3} |C_A|^2 |\langle \sigma \rangle|^2 - 3^{-1/2} (C_V C_A^* + C_A C_V^*) \langle 1 \rangle \langle \sigma \rangle, \quad (4)$$

$$D\xi = i/\sqrt{3} (C_V C_A^* - C_A C_V^*) \langle 1 \rangle \langle \sigma \rangle, \quad (5)$$

where C_V and C_A are the vector and axial-vector coupling constants, respectively, and $\langle 1 \rangle$

and $\langle \sigma \rangle$ are the Fermi and Gamow-Teller matrix elements, respectively. For neutron decay $\langle 1 \rangle = 1$, $\langle \sigma \rangle = +\sqrt{3}$, while for Ne^{19} decay $\langle 1 \rangle \cong 1$, $\langle \sigma \rangle = -1.46 \pm 0.08$.^{5,6}

In Eqs. (3)-(5), corrections due to final-state interactions are neglected. In this approximation a term of the form $\vec{I} \cdot [(\vec{v}/c) \times \hat{q}]$ is odd under time reversal. A precise measurement of D then provides a sensitive test of T invariance, since $D \propto \sin\varphi$ (with $C_A/C_V = re^{i\varphi}$) and T invariance implies that C_A/C_V is real ($\varphi = 0^\circ$ or 180°). Although Coulomb effects might contribute a finite amount to D even if T invariance holds, the Coulomb correction to D vanishes to first order in $Z\alpha/p$ for V or A coupling.³ (Here Z is the atomic number of the final nucleus.)

Neutron beta-decay experiments⁷ yielded the results

$$A(n) = -0.11 \pm 0.02, \quad (6)$$

$$B(n) = 0.88 \pm 0.15, \quad (7)$$

$$D(n) = 0.04 \pm 0.05. \quad (8)$$

These imply $\varphi = 175^\circ \pm 6^\circ$, consistent with T invariance. We have measured $B(\text{Ne}^{19})$ and $D(\text{Ne}^{19})$ by observations of $e^+ - \text{F}^{19-}$ delayed coincidences from decays in flight of a nuclear-spin-polarized atomic beam of Ne^{19} , and have also verified previous measurements^{5,6} of the beta-decay asymmetry $A(\text{Ne}^{19}) = -0.033 \pm 0.002$. The new results are

$$B(\text{Ne}^{19}) = -0.90 \pm 0.13, \quad (9)$$

$$D(\text{Ne}^{19}) = +0.002 \pm 0.014. \quad (10)$$

The values of A , B , and D for Ne^{19} imply $\varphi = 180.2^\circ \pm 1.6^\circ$, again consistent with T invariance.

Ne^{19} is produced in the reaction $\text{F}^{19}(p, n)\text{Ne}^{19}$ at the Berkeley 88-inch cyclotron using a target containing SF_6 gas.^{5,8} The Ne^{19} is continuously separated from the SF_6 and delivered to an atomic-beam source at 30°K , from which it effuses in the 1S_0 ground state. The beam

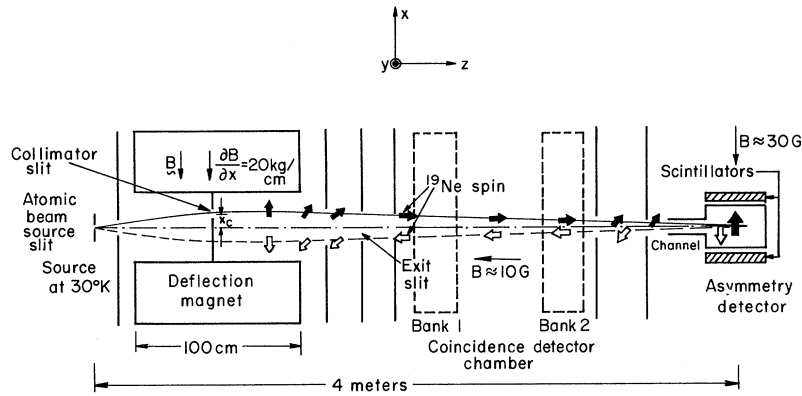


FIG. 1. Schematic diagram of Ne^{19} atomic-beam apparatus, with spin and magnetic field orientations as employed for D experiment. Beam deflections and slit widths are grossly exaggerated for pictorial clarity. The centers of $M_I = \pm \frac{1}{2}$ beams in the coincidence detector chamber are separated by less than 0.05 cm.

is made 25 times as intense by recirculating the radioactive gas through the source.

A conventional "Stern-Gerlach" deflection magnet,⁹ a movable collimating slit, and a fixed exit slit (see Fig. 1) are used to select either of the states $M_I = \pm \frac{1}{2}$. Polarizations of approximately 0.8 are achieved in the coincidence detector chamber as confirmed by observations of the beam-deflection pattern. The polarized-beam flux in this chamber is $\approx 3 \times 10^8$ atoms/sec.

The beam path terminates in the asymmetry detector (see Fig. 1), a short cylinder with a long, narrow channel entrance and thin end walls with adjacent scintillation counters. The asymmetry detector monitors the beam intensity and polarization continuously. The Ne^{19} atoms remain in the cylinder for about 2 sec. Although they make about 10^4 wall collisions in this time, their nuclear polarization is maintained parallel to the cylinder axis, and we observe the A asymmetry in positron emission by atoms decaying in the cylinder.

To measure $D(Ne^{19})$, the spin orientation of beam atoms in the coincidence detector chamber is maintained in the z direction. For measurements of B , the polarization is maintained in the x direction over the entire flight path from deflection magnet to asymmetry detector.

The coincidence chamber houses two detector banks, each containing four positron detectors and four ion detectors spaced alternately 45° apart in the xy plane (see Fig. 2). The positron detectors are conventional scintillation counters with discriminator thresholds set to accept positrons with kinetic energies of 0.7 MeV, or greater. (The maximum e^+ kinetic

energy is 2.24 MeV.)

The recoil F^{19-} ions possess kinetic energies in a continuous range from zero to 219 eV^{10} (as compared with 0.003 eV for Ne^{19} beam atoms). Recoil ions drift from the beam axis to the inner grid (see Figs. 2 and 3), are accelerated to 9 keV, and enter secondary-emission detectors described elsewhere.¹¹ The drift region enclosed by the inner grid is electric-field free. A weak magnetic field imposed to

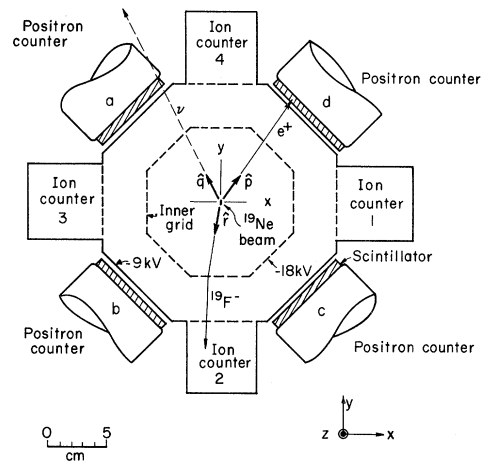


FIG. 2. Schematic diagram of one coincidence detector bank. The Ne^{19} atomic beam moves in the $+z$ direction along the center axis. In the D experiment \hat{I} is parallel or antiparallel to the beam. In the B experiment \hat{I} lies along the x axis to left or right. Most F^{19-} recoils require between 1.6 and $3.1 \mu\text{sec}$ to drift from beam axis to inner grid. The length of the detector region perpendicular to the page is 5 cm. A typical $d-2$ event is shown, with \hat{p} , \hat{q} , and \hat{r} unit vectors in directions of positron, neutrino, and recoil ion, respectively.

Table I. Arrangement of coincidence pairs for *B* and *D*.

<i>B</i> ^a		<i>D</i>	
Spin along <i>x</i> axis	Spin along beam axis	Spin along <i>x</i> axis	Spin along beam axis
Pair	"Image" pair	Pair	"Image" pair
<i>a</i> -2	<i>d</i> -2	<i>a</i> -2	<i>a</i> -1
<i>b</i> -4	<i>c</i> -4	<i>b</i> -1	<i>b</i> -4
<i>c</i> -3*	<i>b</i> -1*	<i>c</i> -4	<i>c</i> -3
<i>d</i> -3*	<i>a</i> -1*	<i>d</i> -3	<i>d</i> -2

^aPairs marked with asterisk have a slightly different geometry factor G_B from those which are unmarked [see Eq. (12), text]. All *B* data are corrected for a small contribution from *A* ($\approx 3\%$).

define the axis of spin polarization has negligible effect on the trajectories of the decay products. The detector arrangement shown in Fig. 2 has the advantage that many possible systematic errors that might otherwise be introduced into the data cancel to high order because of the four-fold symmetry. The cross-sectional dimensions of the beam (1.0 cm \times 0.25 cm) are negligibly small compared to the linear dimensions of the coincidence counter assembly.

During observation of coincidences the polarization is reversed every ten minutes by translating the collimating slit 0.1 cm. (See Fig. 1.) For each run (typically ≈ 50 -h duration) the total number of coincidences obtained with each polarization (collimating slit + or -) is corrected for background. The chief source of background is decay of residual Ne¹⁹ gas in the detector chamber; this contributes $\approx 30\%$ to the over-all counting rate.

We define a quantity Δ , given by

$$\Delta = \frac{1}{2} \left\{ \frac{n' - n}{n' + n} \right\}_{x(c) > 0} - \left\{ \frac{n' - n}{n' + n} \right\}_{x(c) < 0} \right\}, \quad (11)$$

Table II. Summary of *D* data.

Magnetic field directions (See Fig. 1)					
Run No.	Deflection field	Axial field in coincidence detector chamber	Spin polarization for $x(c) > 0$	No. of coincidence counts (corrected)	<i>D</i>
2	+ <i>x</i>	+ <i>z</i>	- <i>z</i>	5980	+0.012 \pm 0.037
3	- <i>x</i>	+ <i>z</i>	- <i>z</i>	5563	-0.022 \pm 0.028
4	- <i>x</i>	- <i>z</i>	+ <i>z</i>	3355	-0.007 \pm 0.047
5	- <i>x</i>	+ <i>z</i>	- <i>z</i>	5281	+0.010 \pm 0.031
6	+ <i>x</i>	- <i>z</i>	+ <i>z</i>	6889	-0.024 \pm 0.049
Total counts (corrected)				30127	
Weighted average					+0.002 \pm 0.014

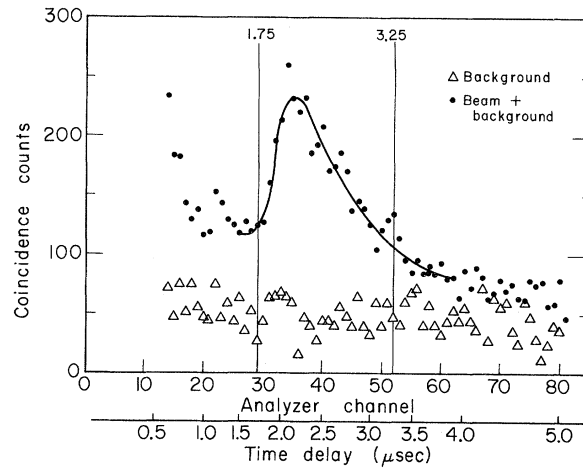


FIG. 3. Positron-recoil-ion coincidence counts versus delay time, as obtained with 4 coincidence pairs. The solid curve is computed from the geometry and the theoretical ion energy distribution as obtained from Eq. (1) in the text, and includes a correction for decay of residual Ne¹⁹ gas in the coincidence detector chamber. The points are experimental. Coincidences in the range 1.75-3.25 μ sec are used in the *B* and *D* experiments.

where n is the corrected coincidence count of a pair and n' is that of its "image" (see Table I and Fig. 2), and $x(c)$ is the collimator position. The two terms in Δ correspond to opposite polarizations. The average of the Δ 's for all pairs employed is called $\bar{\Delta}$. We obtain *B* and *D* from the formulas

$$B = \bar{\Delta}_B (PSG_B)^{-1}, \quad (12)$$

$$D = \bar{\Delta}_D (PSG_D)^{-1}. \quad (13)$$

Here P is the polarization, $S = 0.85 \pm 0.1$ is a

correction for positron backscattering from chamber walls, etc., into the positron counters,¹² and $G_B \cong 0.6$ and $G_D \cong 0.75$ are geometry factors arising from finite detector solid angles, etc. The geometry factors have been calculated to a few percent precision.

The uncertainty in B arises primarily from that in P , S , and the background correction. The uncertainty in D is due almost wholly to the statistical uncertainty in $\bar{\Delta}_D$ (standard error in the mean). Table II is a summary of our results for D , run by run.

A detailed report of the present work will shortly be submitted to the Physical Review.

It is a pleasure to acknowledge the encouragement and support we have received from Professor B. Harvey, Professor E. Segrè, Professor H. Shugart, Professor R. L. Thornton, and others. We are indebted to D. Macdonald, D. Landis, D. Lundgren, J. Meneghetti, and many others for excellent technical work in our behalf.

†Research supported by the U. S. Atomic Energy Commission.

*Alfred P. Sloan Fellow.

¹J. H. Christenson, J. W. Cronin, V. L. Fitch, and R. Turlay, Phys. Rev. Letters **13**, 138 (1964).

²See, for example, J. Bernstein, G. Feinberg, and T. D. Lee, Phys. Rev. **139**, B1650 (1965).

³J. D. Jackson, S. B. Treiman, and H. W. Wyld, Nucl. Phys. **4**, 206 (1957).

⁴See, for example, E. J. Konopinski, The Theory of Beta Radioactivity (Clarendon Press, Oxford, 1966), p. 9.

⁵The experimental value of $\langle\sigma\rangle$ for Ne¹⁹ as determined from $A(\text{Ne}^{19})$ is given by D. A. Dobson, University of California Radiation Laboratory Report No. UCRL-11169, 1963 (unpublished).

⁶For $\langle\sigma\rangle$ of Ne¹⁹, see also F. P. Calaprice, E. D. Commins, and D. A. Dobson, Phys. Rev. **137**, B1453 (1965).

⁷M. T. Burgy, V. E. Krohn, T. B. Novey, G. R. Ringo, and V. L. Telegdi, Phys. Rev. **120**, 1829 (1960). See also M. A. Clark and J. M. Robson, Can. J. Phys. **38**, 693 (1960); **13** (1961).

⁸E. D. Commins and D. A. Dobson, Phys. Rev. Letters **10**, 347 (1963).

⁹See, for example, N. F. Ramsey, Molecular Beams (Clarendon Press, Oxford, 1956), p. 399.

¹⁰J. S. Allen *et al.*, Phys. Rev. **116**, 134 (1959).

¹¹H. M. Gibbs and E. D. Commins, Rev. Sci. Instr. **37**, 1385 (1966).

¹²A. Bisi and L. Braicovich, Nucl. Phys. **58**, 171 (1964).

SEARCH FOR A Y_2^* RESONANCE IN THE $\Sigma^-\pi^-$ CHANNEL*

Robert B. Bell, Robert P. Ely, and Yu-Li Pan†

Lawrence Radiation Laboratory, University of California, Berkeley, California

(Received 21 April 1967)

We have examined the reaction $K^- + d \rightarrow \Sigma^- + \pi^+ + \pi^- + p$ in the K^-n c.m. energy range from 1660 to 1900 MeV in an attempt to confirm the existence of the $Y_2^*(1415)$ reported previously by two of us.¹ The evidence for this isobar was based on a study of the reaction $K^- + n$ (carbon) $\rightarrow \Sigma^- + \pi^+ + \pi^-$ in a heavy-liquid chamber. If such a Y_2^* exists, it would be the only confirmed candidate for the 27-plet of SU(3). In the present experiment K^- mesons with incident momenta of 815, 915, 1015, and 1115 MeV/c interacted in the University of California Lawrence Radiation Laboratory 25-inch deuterium bubble chamber. The experimental details were reported in a previous Letter,² in which it was shown that the dominant reaction in this channel at these energies is $K^- + n \rightarrow Y_1^*(1760) \rightarrow Y_0^*(1520) + \pi^- \rightarrow \Sigma^- + \pi^+ + \pi^-$.

The Dalitz plot of Fig. 1 shows that the $Y_0^*(1520)$

is produced copiously throughout the majority of the available energy region of this experiment, and therefore this isobar will reflect strongly into the $\Sigma^-\pi^-$ mass spectrum. We attempted to remove this reflection in the following manner: As is discussed in Ref. 2, the expected three-body phase space is the sum of phase spaces at each available energy, weighted by the probability that that energy occurs; the probability can be determined from the deuteron wave function. The derived phase space, plus Breit-Wigner curves to describe production of the $Y_0^*(1520)$ and $Y_0^*(1405)$, were combined to give the best fit to the $\Sigma^-\pi^+$ mass plot. In this way we determined the correct percentages of the reflections of these two resonances to remove from the $\Sigma^-\pi^-$ mass spectrum. The resulting distribution, together with the expected three-body phase space, is shown in